



Quantifying COVID-19 importation risk in a dynamic network of domestic cities and international countries

Xiaoyi Han^{a,b}, Yilan Xu^{c,1}, Linlin Fan^d, Yi Huang^e, Minhong Xu^e, and Song Gao^f

^aWang Yanan Institute for Studies in Economics (WISE), Xiamen University, Xiamen 361005, China; ^bSchool of Economics, Xiamen University, Xiamen 361005, China; ^cDepartment of Agriculture and Consumer Economics, University of Illinois at Urbana-Champaign, Champaign, IL 61820; ^dDepartment of Agricultural Economics, Sociology, and Education, Pennsylvania State University, Philadelphia, PA 16802; ^eInstitute of Urban Development, Nanjing Audit University, Nanjing 211815, China; and ^fGeospatial Data Science Lab, Department of Geography, University of Wisconsin-Madison, Madison, WI 53706

Edited by Douglas S. Massey, Princeton University, Princeton, NJ, and approved June 14, 2021 (received for review January 8, 2021)

Since its outbreak in December 2019, the novel coronavirus 2019 (COVID-19) has spread to 191 countries and caused millions of deaths. Many countries have experienced multiple epidemic waves and faced containment pressures from both domestic and international transmission. In this study, we conduct a multiscale geographic analysis of the spread of COVID-19 in a policy-influenced dynamic network to quantify COVID-19 importation risk under different policy scenarios using evidence from China. Our spatial dynamic panel data (SDPD) model explicitly distinguishes the effects of travel flows from the effects of transmissibility within cities, across cities, and across national borders. We find that within-city transmission was the dominant transmission mechanism in China at the beginning of the outbreak and that all domestic transmission mechanisms were muted or significantly weakened before importation posed a threat. We identify effective containment policies by matching the change points of domestic and importation transmissibility parameters to the timing of various interventions. Our simulations suggest that importation risk is limited when domestic transmission is under control, but that cumulative cases would have been almost 13 times higher if domestic transmissibility had resurged to its precontainment level after importation and 32 times higher if domestic transmissibility had remained at its precontainment level since the outbreak. Our findings provide practical insights into infectious disease containment and call for collaborative and coordinated global suppression efforts.

COVID-19 | mobility networks | importation risk | spatial dynamic panel data model | spatiotemporal analysis

Since its outbreak in December 2019, the novel coronavirus disease (COVID-19) has spread to 191 countries in the world, resulting in over 129 million confirmed cases and more than 2.8 million deaths worldwide by 31 March 2021 (1). Many countries had experienced multiple epidemic waves since the initial outbreak of COVID-19. As COVID-19 is spreading around the globe, countries need to manage both domestic spread and international importation risks at the same time, with the relative magnitudes of these threats varying over time. However, to the best of our knowledge, few studies have investigated the effectiveness of containment strategies for COVID-19 accounting for both domestic and international threats (2, 3). Our study fills in the research gap by quantifying COVID-19 importation risk under different policy scenarios using evidence from China during its transition from an infectious disease exporting country to an importing country.

COVID-19 transmits mainly through close contact with infected patients (4). Thus, both domestic and international population movements pose a great threat to the containment of the disease. Studies have shown that travel flows explained the initial spread from Wuhan to other cities in China (5–7), from China to other countries (8, 9), from city to city in other countries (10), and from neighborhood to neighborhood in a city (11–13). Meanwhile, many countries have also long recognized the importance of managing importation risk in containing COVID-19

spread; 89 countries and regions implemented travel restrictions during the first 5 mo of the pandemic (14). However, a multiscale analysis is lacking in existing COVID-19 studies to integrate both domestic and international spread in a policy-influenced dynamic network. Previous epidemiological literature has integrated short-distance commuting flows with long-distance airline traffic flows to simulate the spread of a hypothetical pandemic influenza (15), yet the intensities of disease transmission at multiple scales cannot be estimated under the framework of current epidemiological models. Built on a spatial-social network of 284 Chinese cities including Wuhan and 48 countries and regions with direct flights to mainland China, our study explicitly quantifies the magnitudes of various transmission channels, especially the importation risk, and evaluates the effectiveness of multiple containment policies.

When the World Health Organization (WHO) declared COVID-19 a pandemic on 11 March 2020, China transitioned from an infectious disease exporting country to an importing country. Since then, China has continued its containment efforts in the face of infections imported through inbound international flights. In March, a series of policies took effect to control international travel flows, including a ban on admission of foreigners and the “five one” policy that restricted both international flight frequency and seat capacity. Additionally, policies intending to lower the number and transmissibility of imported cases included

Significance

In the COVID-19 pandemic, countries need to manage both the domestic spread and the spread of the virus from foreign countries, with their relative urgency varying over time. Based on a dynamic network of cities and countries connected by travel flows, we demonstrate that imported cases would have a limited effect on a country's confirmed cases if domestic transmission mechanisms had been muted or significantly weakened. However, uncontrolled domestic disease transmission can fuel the spread from abroad to domestic. We show that domestic transmissibility controls should be prioritized over travel restrictions and international transmissibility controls to limit the virus spread from abroad. Our research sheds light on the proper timing to reopen borders under different domestic disease control scenarios.

Author contributions: Y.X. conceptualized the research idea and directed the project; X.H. performed the estimations and simulations; L.F. collected intervention policies and suggested the design of some simulations; Y.H., M.X., and S.G. collected and processed data; Y.X. wrote the manuscript; X.H. and S.G. obtained the funding; and all authors provided edited versions of the paper and helped shape the research, analysis, result visualization, and manuscript.

The authors declare no competing interest.

This article is a PNAS Direct Submission.

Published under the PNAS license.

¹To whom correspondence may be addressed. Email: yilanxu@illinois.edu.

This article contains supporting information online at <https://www.pnas.org/lookup/suppl/doi:10.1073/pnas.2100201118/-/DCSupplemental>.

Published July 20, 2021.

the 14-d preregistration of health status and negative nucleic acid test and antibody test results prior to departure, as well as mandatory testing and 14-d centralized quarantine upon arrival. Before March, China had focused on the containment of domestic spread. It took aggressive approaches to limit domestic travel flows at the outbreak of the disease (7, 16–19); a total of 80 cities in 22 provinces were under complete or partial lockdowns by 29 February 2020 (20). China also took proactive nonpharmaceutical interventions to lower the transmissibility of the disease. These efforts included mask mandates, check points and quarantine zones, closed management of communities, family outdoor restrictions, delayed school opening for the spring semester, and fast testing (see *SI Appendix* for a chronicle of the policies). These policies could also raise the awareness of the infection risk and induce health behavioral changes for self-protection. On 18 March, China claimed zero new local cases, and for the first time all new cases were imported. Combining the efforts at the domestic and international fronts, by the end of our sampling period on 28 April 2020, a total of 82,858 cases were confirmed, among which 50,333 were confirmed in Wuhan and 1,660 were imported (21). By the end of March 2021, a total of 90,217 COVID-19 cases were confirmed, among which 50,357 were confirmed in Wuhan and 5,300 were imported (22, 23).

What explains China's trajectory in containing COVID-19 in the face of the initial threat from the earlier epicenter and the later threat from importation? To what extent can its experience benefit other countries? To answer these questions, it is vital to examine the mechanisms, dynamics, and interactions of COVID-19 transmission at multiple geographic scales as it spreads within cities, across cities, and across national borders. In this study, we model the spread of COVID-19 in a policy-influenced dynamic spatial–social network. Using China's large-scale mobility data and international flight data, we construct an integrated network of 284 Chinese cities and 48 countries and regions accounting for the dynamic effects of travel restriction policies. Using a spatial dynamic panel data (SDPD) model, we explicitly characterize different infectious disease transmission mechanisms, including within-city, across-city, and cross-border transmission. Under the SDPD framework, transmissibility interventions influence the parameters of these transmission mechanisms, whereas travel restrictions influence the structure of the spatial–social network. We adopt a Bayesian approach to allow the model to identify the change point of each transmission mechanism (24). By introducing parameter-specific change points for domestic and international transmissibility, our work extends the current SDPD models with constant coefficients (25, 26) and those with only one common structural break for all parameters (27). We then compare the change points with the timing of various containment policies to identify effective containment policies. We further run simulations to quantify the counterfactual cumulative number of cases under different scenarios when an importation threat is present:

$$\begin{aligned}
 Y_t = & \underbrace{\lambda(t)\bar{W}_t Y_t}_{\text{cross-city transmission}} + \underbrace{\gamma(t)M_{wh,t} Y_{wh,t}}_{\text{Wuhan influence}} + \underbrace{\rho(t)Y_{t-1}}_{\text{within-city transmission}} \\
 & + \underbrace{\mu(t)\bar{W}_{t-1} Y_{t-1}}_{\text{diffusion effect}} + \underbrace{B_t \delta(t)}_{\text{importation}} + \underbrace{\xi_t \phi(t)}_{\text{domestic inflow}} \\
 & + \underbrace{X_t \beta_1}_{\text{weather variable}} + \underbrace{C \beta_2}_{\text{number of hospital, provincial effect and other controls}} \\
 & + \underbrace{l_n \alpha_t}_{\text{time effect}} + \underbrace{U_t}_{\text{disturbances}}, \quad t = 1, 2, \dots, T. \quad [1]
 \end{aligned}$$

Materials and Methods

Data. We obtain the city-level daily newly COVID-19 confirmed cases data for the period 20 January 2020 to 28 April 2020 from the China Data Labo-

ratory (28). We supplement the data with information released by Chinese local health commissions and news reports to generate total newly confirmed cases for the baseline model and domestic newly confirmed cases for robustness checks. We obtain the country-level daily newly confirmed cases data for the same period from the European Center for Disease Prevention and Control (29). Acknowledging the average of a 5-d incubation period of COVID-19 (30), we use the intercity daily travel inflow distributions from Baidu *Qianxi* (Baidu Mobility) between 13 January 2020 and 25 April 2020 for 284 cities in China to construct the domestic city network (31). To construct the connections with 48 countries and regions with direct flights to mainland China, we exploit the international flight information from the OpenFlights website supplemented with the Aviation Edge data for the routes with missing origin or destination information. We use the Baidu Mobility data and international flight data for the same period in the 2019 lunar calendar as proxies for the unrestricted travel flows of 2020. We also construct control variables including weather conditions, gross domestic product, population, and the numbers of hospitals and doctors from multiple sources. We describe detailed data sources and variable construction in *SI Appendix*.

To illustrate the dynamic policy influence on the travel network and the evolution of confirmed cases, we provide two snapshots in Fig. 1. Fig. 1A plots the daily averages of confirmed cases in 44 Chinese cities with international airports, their domestic travel flows into Beijing, and their inbound international flights over 1 to 23 January 2020, the period before Wuhan's lockdown. Fig. 1B plots the same information for 24 January to 15 February 2020. Compared with Fig. 1A, Fig. 1B shows more confirmed cases, less intense domestic travel flows, and fewer international flights after Wuhan was locked down and multifaceted containment policies took effect. In our analytical sample, we include 284 Chinese cities including those without an international airport to account for the full network integrated by domestic travel flows and international flights.

A Spatial Dynamic Panel Data Model. We specify the following SDPD model (Eq. 1) to distinguish between four domestic transmission mechanisms and the international transmission. The variable Y_t is the total daily newly confirmed cases for 283 Chinese cities with available data but excluding Wuhan. Wuhan as the early epicenter is modeled as a regressor with its daily newly confirmed cases of $y_{wh,t}$. The spatial weights matrix, \bar{W}_t , represents the domestic travel network constructed from 5-d lagged average travel flow distributions between cities. The share of travel inflow to a city from Wuhan is denoted as $M_{wh,t}$. Thus, the four domestic transmission mechanisms are cross-city transmission, $\lambda(t)$, i.e., the spillover effects across cities; the spillover effect from the epicenter of Wuhan, $\gamma(t)$; the within-city transmission, $\rho(t)$, i.e., the persistence effect; and the diffusion effect of transmission, $\mu(t)$. To model the international transmission, we include B_t , the daily abroad infection indexes constructed from foreign countries' daily newly confirmed cases and their direct flights to Chinese cities. Hence, $\delta(t)$ measures the international transmission effect. Our innovation to the existing SDPD literature is to allow different change points for each of the transmissibility parameters, which are identified by a Bayesian approach as described in *SI Appendix*.

In addition to the above transmission mechanisms of interest, we also control for the scale effect of travel inflow into a city (ξ_t), time-varying and time-invariant control variables (X_t and C , respectively), and the day fixed effects ($l_n \alpha_t$). Several of these variables help control for the potential underreporting of confirmed cases. For instance, city-level numbers of various types of hospitals serve as a proxy for healthcare resources, especially the COVID-19 testing capacity. The day fixed effects control for the time-varying yet systematic reporting pattern at the national level. The province fixed effects account for time-invariant province-specific unobservables related to systematically underreporting at the province level. We specify a normal distribution for the dependent variable because the reported newly confirmed cases can be negative on some days due to changes in reporting standard and periodic adjustments, which are partially controlled by the day fixed effects. As robustness checks, we also run alternative model specifications where we use different travel flow lags, weight the travel distributions by travel flows, and allow spatial heterogeneity or a Poisson distribution for some subsamples. All robustness checks are reported in *SI Appendix*.

Results

Two Episodes of COVID-19 Spread in China. We begin by examining the magnitude of each transmission mechanism and the associated change points. Fig. 2 plots the levels and change

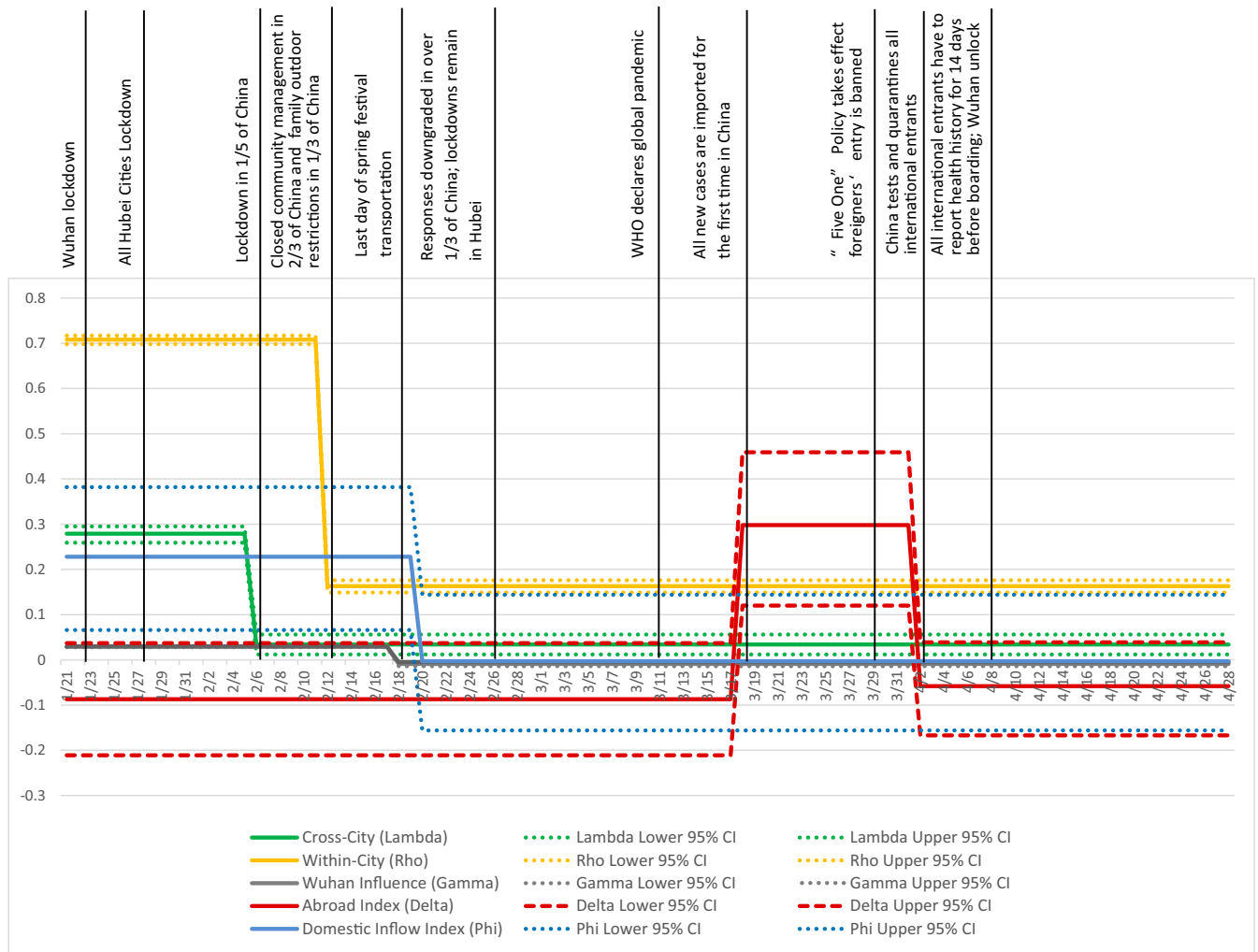


Fig. 2. The timeline of various containment policies in China and the change points in the coefficients for within-city transmission, cross-city transmission, Wuhan influence, domestic flow influence, and abroad infection index.

transmission was the dominant mechanism with a coefficient of 0.708 (95% CI: 0.698 to 0.717), followed by the cross-city transmission with a coefficient of 0.279 (95% CI: 0.259 to 0.295). Somewhat surprising is the limited spillover effect from Wuhan, which had a coefficient of 0.029 (95% CI: 0.028 to 0.030). It was likely due to the extra stringent screening and quarantine targeting the travel flows from Wuhan to other cities. The coefficient of the diffusion effect was insignificant throughout the sampling period and thus not included in Fig. 2. The coefficient of the inflow travel volume was positive and significant only at the initial stage, yet the magnitude was not comparable with the above mechanisms due to the different units of the explanatory variables.

The change points identified by the Bayesian approach matched the timing of the respective containment policies. On 6 February 2020, the cross-city transmission decreased from 0.279 (95% CI: 0.259 to 0.295) to 0.034 (95% CI: 0.012 to 0.056), corresponding with the stringent interventions targeting cross-city transmissibility at the outbreak. Besides the complete and partial lockdowns in 22 cities, checkpoints and quarantine zones were implemented in over one-fifth of Chinese cities by 6 February. The within-city transmission coefficient declined sharply from 0.708 (95% CI: 0.698 to 0.717) to 0.163 (95% CI: 0.149 to 0.176) on 12 February. This change reflected the effects of interventions

on the within-city transmissibility. Closed community management was enforced in over two-thirds of Chinese cities, and family outdoor restrictions were in place in one-third of Chinese cities by 12 February (*SI Appendix*). Finally, the coefficient of domestic inflows on new COVID-19 cases was statistically significant until 19 February. The significant but brief effect matched the massive population movement and intense contacts during the Spring Festival travel rush (*Chunyun* in Chinese) that ended on 18 February.

On the international front, since the WHO declared the global pandemic on 11 March 2020, imported cases had increased dramatically in China. However, with timely and effective policies, transmissibility from imported cases quickly declined. On 18 March 2020, the coefficient of the abroad infection index increased from insignificant to 0.298 (95% CI: 0.120 to 0.459), corresponding to the day when all new cases in China were imported. The coefficient returned to insignificant on 2 April. The short-lived importation effects reflected the intense efforts to lower the transmissibility from imported cases and to reduce international travel flows. Mandatory testing at customs was required starting on 23 March at the four largest international flight hubs—Beijing, Shanghai, Guangzhou, and Shenzhen. Ban on foreigners' entry and the "five one" international flight restrictions were implemented on 28 and 29 March, respectively.

By 1 April, mandatory testing and centralized quarantine for at least 14 d were required at all international airports in China (*SI Appendix*). With these importation containment policies, the transmissibility from imported cases was significantly abated.

Limited Importation Risk When Domestic Transmission Was under Control. We further run simulations under different scenarios to quantify the isolated effects of the importation transmissibility, international travel flows, domestic transmissibility, and domestic travel flows. Fig. 3 plots the cumulative cases outside of

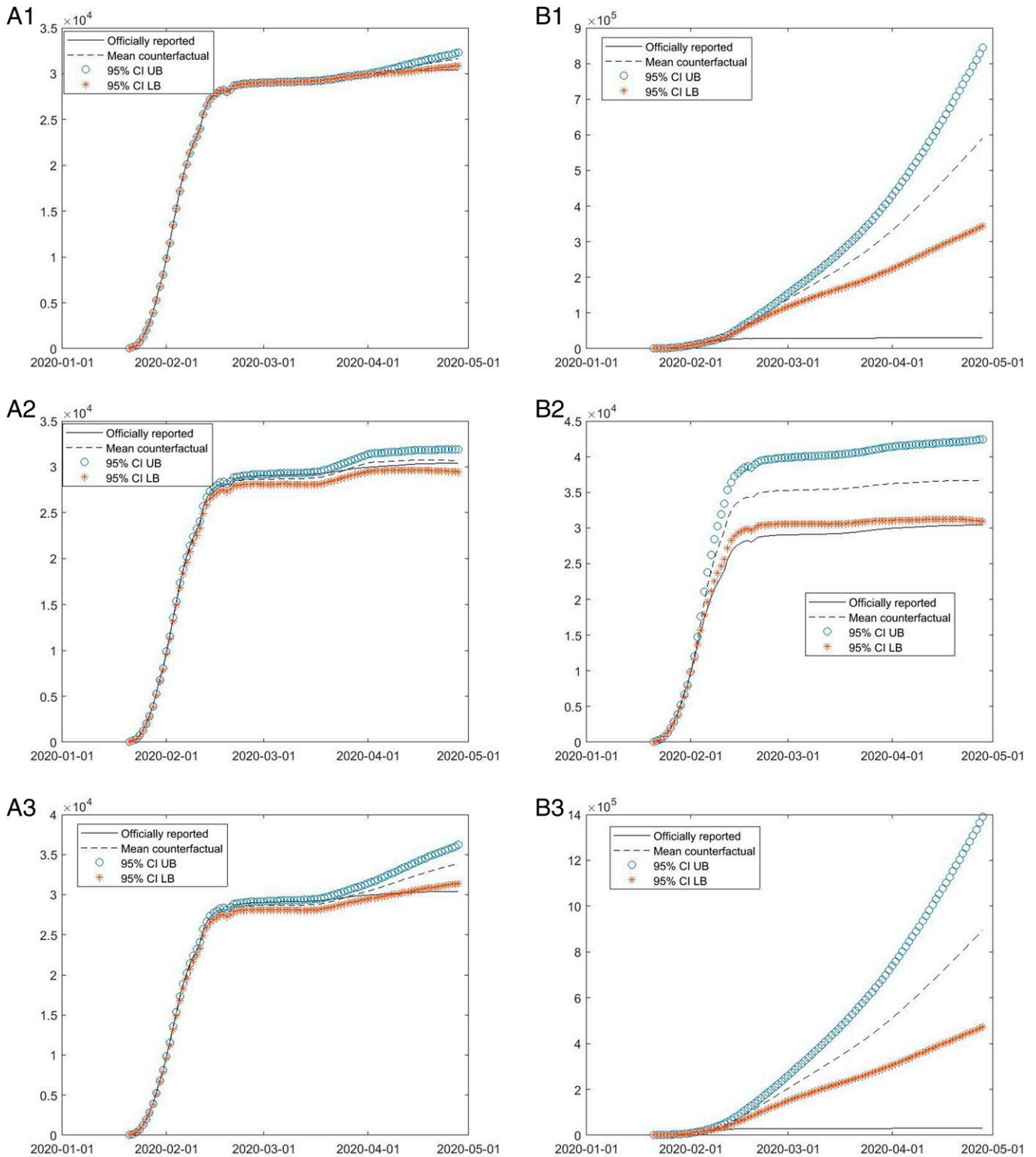


Fig. 3. Simulated cumulative cases outside of Wuhan in the scenario when effects of transmission and effects of travel flows can be isolated. In *A1* (*B1*), the importation (domestic) transmissibility remained high since its emergence. In *A2* (*B2*), the international (domestic) travel flows were unrestricted at the 2019 level. In *A3* (*B3*), both the importation (domestic) transmissibility remained high and the international (domestic) travel flows were unrestricted. UB, upper bound; LB, lower bound.

Wuhan by the end of April 2020 in six scenarios. In Fig. 3 A1, we allow the importation transmissibility parameter to remain at its highest level since emergence, with everything else unchanged. In Fig. 3 A2, we replace the 2020 international travel flows with the 2019 level to mimic the unrestricted international travel throughout the sample period, with everything else unchanged. In Fig. 3 A3, we allow both importation transmissibility to remain at its highest level since emergence and international travel flows to be unrestricted throughout the sample period. Compared to the actual 30,406 cumulative cases in these 283 cities (excluding Wuhan) by 28 April 2020 (solid lines), the counterfactual cumulative cases (dashed line) would have been 1,244 (or 4.1%) more under the high importation transmissibility, 284 (or 0.9%) more under the unrestricted international travel flows, and 3,504 (or 11.5%) more under both high importation transmissibility and unrestricted international travel flows. These patterns suggest that importation transmissibility and international travel flows had relatively small effects on COVID-19 transmission in China. A critical reason for the limited importation risk was that the domestic transmission mechanisms had been muted or significantly weakened when importation took place, which limited the onward transmission of imported disease. Meanwhile, when we run similar scenarios for the domestic transmission mechanisms holding the importation mechanisms as factual, the

cumulative cases by the end of April would have been 18.44 times higher if the domestic transmissibility had remained high (Fig. 3 B1), only 20.6% higher if domestic travel flows remained unrestricted (Fig. 3 B2), and 28.50 times higher under both high domestic transmissibility and unrestricted domestic flows (Fig. 3 B3). Our simulation results suggest that domestic transmission mechanisms play a more important role than importation in COVID-19 spread. Moreover, high domestic transmissibility is a greater threat than unrestricted domestic travel flows, implying the importance of reducing domestic transmissibility through various intervention measures.

Moderate Importation Risk with Partially Resurged Domestic Transmissibility. To provide more practical insights on COVID-19 containment, we now integrate importation with domestic transmission and simulate the cumulative number of cases when domestic transmissibility was first contained and then resurged after importation emerged. When the importation risk arose, domestic transmission mechanisms could presumably become more intense because of higher pressure from the international front. Although it did not happen in China due to the stringent importation control policies, it is a worthwhile case to consider for other countries. The simulation results are presented in Fig. 4. In all scenarios, we assume that the importation

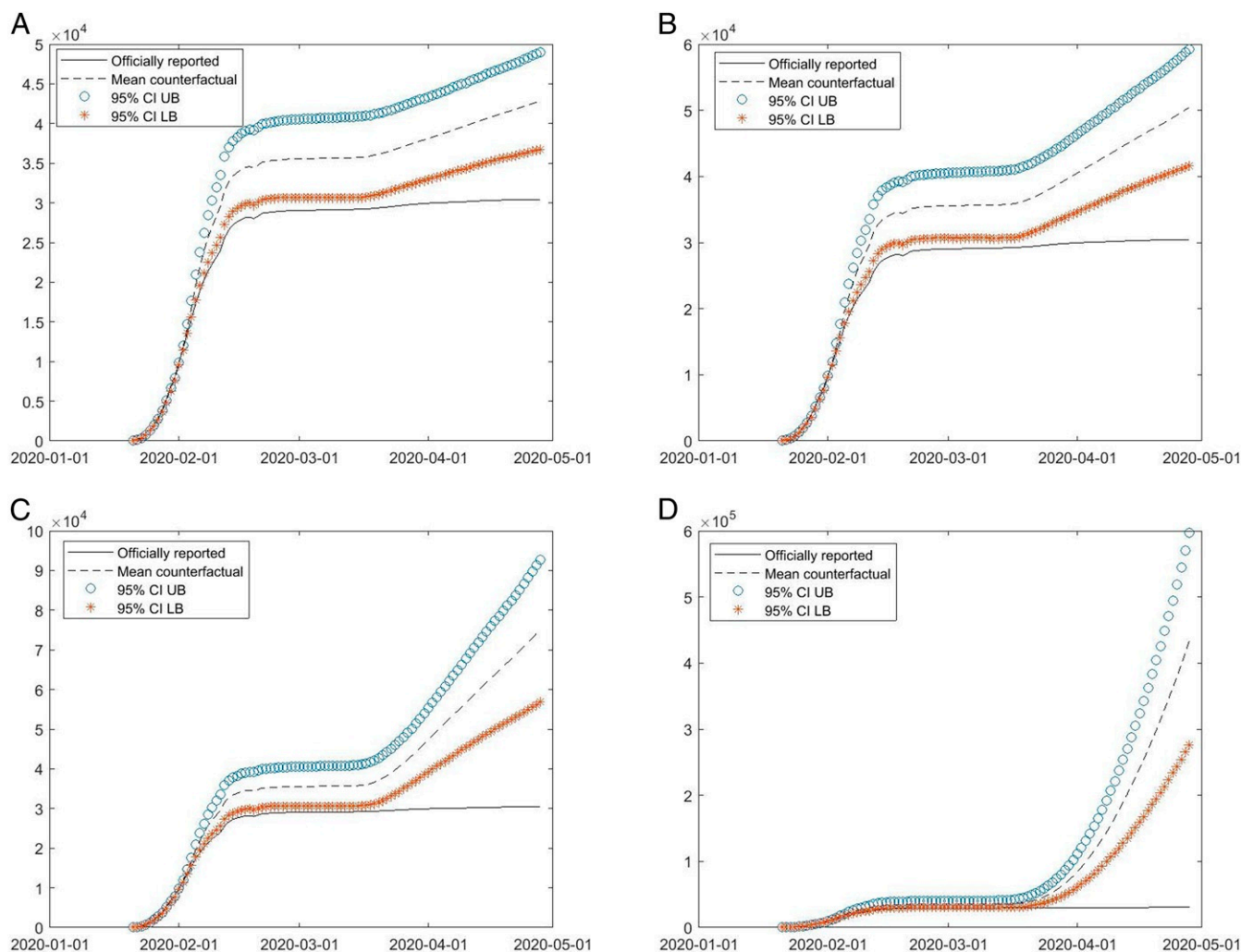


Fig. 4. Simulated cumulative cases outside of Wuhan in the scenario when domestic transmission resurged after importation. In A–D, the domestic transmissibility parameters changed to 25, 50, 75, 100% of their precontainment levels after importation emerged, respectively, while the importation transmissibility remained high since its emergence and international and domestic travel flows were both unrestricted. UB, upper bound; LB, lower bound.

transmissibility remained high since its emergence and international travel flows were unrestricted throughout the sampling period. Given the finding that domestic travel flows had a smaller effect than domestic transmissibility on COVID-19 spread, we also assume that domestic travel flows were unrestricted. We simulate four scenarios by changing the domestic transmissibility parameters to 25, 50, 75, 100% of their precontainment levels (Fig. 4 A–D, respectively) after importation arises. In all scenarios, the counterfactual cumulative cases slightly exceeded the factual number initially, which could be explained by unrestricted domestic travel flows. However, the gap remained constant after the end of the Spring Festival travel rush until importation arose, implying a shock introduced by the rush. After importation arose, the COVID-19 spread could have evolved very differently depending on the degree of resurgence in domestic transmissibility. The cumulative number of cases by the end of April would have been 40.89, 65.95, 147.35% higher if domestic transmissibility parameters resurged to 25, 50, and 75% of their precontainment level, respectively (Fig. 4 A–C). When the domestic transmissibility resurged to 100% of its precontainment level, the cumulative cases would have been almost 13 times higher than the factual cases (Fig. 4D). The simulation results suggest that importation risk was only moderate when the domestic transmissibility moderately resurged, but that cumula-

tive cases could increase dramatically as domestic transmissibility resurged to its precontainment level.

Remarkably High Importation Risk If Domestic Transmissibility Had Not Been Suppressed before Importation. Finally, we consider the case that the domestic transmission was only partially suppressed before importation arose, which is a more realistic case for many countries where some of the radical containment approaches taken by China would have been infeasible. In Fig. 5, we simulate the cumulative number of cases in scenarios where the domestic transmissibility parameters changed to 25, 50, 75, and 100% of their initial levels after their respective change points (Fig. 5 A–D, respectively). Again, we assume unrestricted international and domestic travel flows throughout the sampling period and that the importation transmissibility remained high since its emergence. In all scenarios, the counterfactual cumulative cases exceeded the factual numbers before the importation arose, yet the gap between the factual and counterfactual continued to widen over time due to the combined effects of unrestricted domestic travel flows and the partially suppressed domestic transmissibility. The cumulative number of COVID-19 cases by the end of April would have been 48.52, 101.97, and 256.51% higher if domestic transmissibility had been suppressed to 25, 50, and 75% of its precontainment level, respectively.

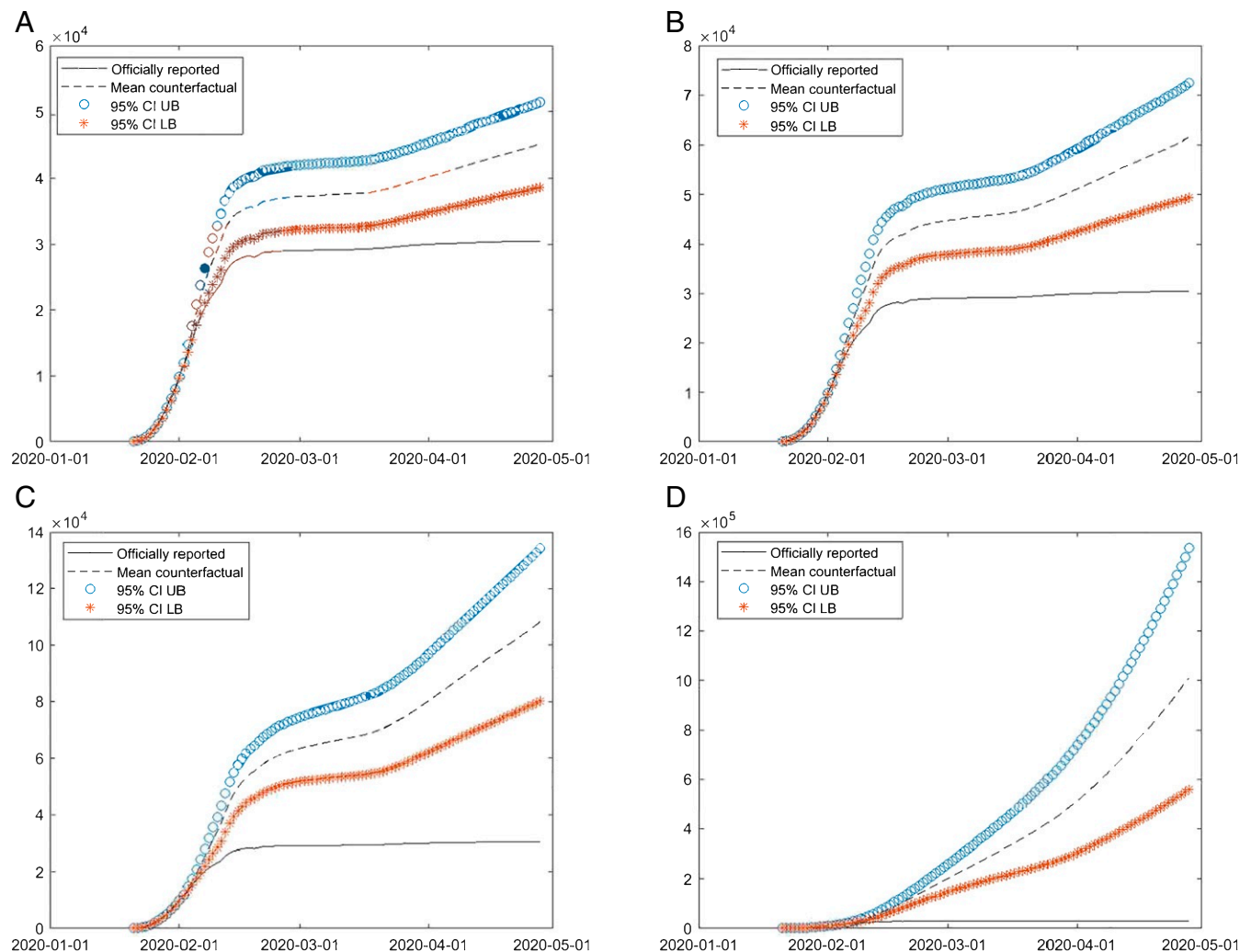


Fig. 5. Simulated cumulative cases outside of Wuhan in the scenario when domestic transmissibility was not suppressed before importation. In A–D, the domestic transmissibility parameters changed to 25, 50, 75, and 100% of their initial levels after the respective change points, respectively, while the importation transmissibility remained high since its emergence and international and domestic travel flows were both unrestricted. UB, upper bound; LB, lower bound.

The cumulative number would have been 32 times higher if domestic transmissibility remained at 100% of its precontainment level. In reality, had domestic transmission remained uncontrolled before the importation hit, domestic transmission parameters would have been even higher than their initial levels as we assumed in Fig. 5D. In this sense, the true importation risk would be even higher than our simulation in Fig. 5D. Compared to the previous case where domestic transmission had been under control before importation, this analysis suggests that importation would have had a much larger effect if domestic transmission had not been under control.

Discussion

COVID-19 containment is a continued effort that requires a dynamic and adaptive perspective. Our model has the advantages of quantifying the magnitudes of various transmission mechanisms and detecting their changes over time. Thus, the model can be used to monitor infectious disease transmission dynamics and to identify threats in real time. Our study shows that imported infectious diseases can propagate to domestic cities via international airports and transmit through multiscale networks. Cities and countries around the world constitute a network with not only a geographic structure but also a social structure shaped by domestic travel (5, 7), migration (32), and friendships (33), as well as international flights (8, 9), shared borders, and trade (34). Thus, the infections and containment policies in one place have not only local effects but also spillover effects across cities and borders through multiscale geographical and social connections (15, 35). Our findings call for collaborative and coordinated global suppression efforts that recognize the spillover effects (35–37).

The control of a pandemic is a complex matter that needs to account for each country's population demographics, socioeconomic status, culture, geography, politics, climate, et cetera. With enormous heterogeneities across countries, there is no "one-size-fits-all" containment strategy that works for all countries. Our study provides a framework to quantify various transmission mechanisms and evaluate the effects of different containment strategies. The country-specific analysis under such a framework can provide operational insights into a country's infectious disease containment. Based on the analysis of the expected relative sizes of imported and domestic cases in 162 countries, scholars have cautioned that countries with low domestic COVID-19 infections are at risk for a second local epidemic wave introduced by international traffic (38). Our study uncovers the mechanisms that make China a counterexample to this conclusion. Our simulations show that even without international travel restrictions and importation transmission controls, imported cases would still

have limited effects on total confirmed cases in China despite its extremely low domestic cases. This is because domestic transmission mechanisms have been muted or significantly alleviated when importation risk arose. Although the aggressive containment policies of China as calibrated in our baseline model may not apply in other countries, our simulations provide more realistic scenarios of what could have happened if a more moderate approach were taken as in other countries. An innovative discovery of our study is that the importation control policies are the most effective when domestic transmissions are at least partially suppressed. Uncontrolled domestic transmissions can exponentially magnify the effects of importation. This insight can guide resource allocation and prioritization when a country adapts its containment strategy as COVID-19 evolves.

Our study further discerns the effectiveness of transmissibility control and travel restriction on both domestic and international fronts. We find that domestic transmissibility interventions are more important than domestic travel flow control, a point that resonates with earlier findings from multiple studies based on epidemiological models. Both domestic and international travel restrictions have been shown to help decrease the confirmed cases and delay the time to outbreak in the destinations (7, 9, 20, 39, 40); however, transmissibility interventions (such as social distancing, testing, and timely quarantine) are more effective than travel restrictions when the disease has already been widespread within a country (41). Travel controls such as lockdowns work more effectively when coupled with reduction in transmissibility (16). Our study provides insights into the international front. It reveals that international transmissibility interventions (e.g., preregistration of health status, double-negative tests, centralized quarantine) also had greater effects than international flight restrictions on containing the spread of COVID-19, although both interventions at the international front would have almost negligible effects if domestic transmissibility interventions were not in place.

Data Availability. Resources for COVID-19 Study (CSV) data have been deposited in Harvard Dataverse (<https://projects.iq.harvard.edu/chinadatalab/resources-covid-19>). All the data that support the findings of this study are publicly available on the GitHub repository under the MIT license (<https://github.com/GeoDS/COVID-SDPD>).

ACKNOWLEDGMENTS. We thank the China Data Laboratory for providing the data for "Resources for COVID-19 Study" (<https://projects.iq.harvard.edu/chinadatalab/resources-covid-19>). X.H. acknowledges the financial support of the National Natural Science Foundation of China (Awards 71973113 and 71988101). S.G. acknowledges the funding support provided by the US NSF (Award BCS-2027375). Any opinions, findings, and conclusions or recommendations expressed in this material are those of the author(s) and do not necessarily reflect the views of the funders.

- E. Dong, H. Du, L. Gardner, An interactive web-based dashboard to track COVID-19 in real time. *Lancet Infect. Dis.* **20**, 533–534 (2020).
- S. Lai et al., Assessing spread risk of Wuhan novel coronavirus within and beyond China, January–April 2020: A travel network-based modelling study. *medRxiv* [Preprint] (2020). <https://www.ncbi.nlm.nih.gov/pmc/articles/PMC7276059/> (Accessed 8 July 2021).
- N. W. Ruktanonchai et al., Assessing the impact of coordinated COVID-19 exit strategies across Europe. *Science* **369**, 1465–1470 (2020).
- M. Klompas, M. A. Baker, C. Rhee, Airborne transmission of SARS-CoV-2: Theoretical considerations and available evidence. *J. Am. Med. Assoc.* **324**, 441–442 (2020).
- M. U. G. Kraemer et al., The effect of human mobility and control measures on the COVID-19 epidemic in China. *Science* **368**, 493–497 (2020).
- J. S. Jia et al., Population flow drives spatio-temporal distribution of COVID-19 in China. *Nature* **582**, 389–394 (2020).
- H. Tian et al., An investigation of transmission control measures during the first 50 days of the COVID-19 epidemic in China. *Science* **368**, 638–642 (2020).
- M. Chinazzi et al., The effect of travel restrictions on the spread of the 2019 novel coronavirus (COVID-19) outbreak. *Science* **368**, 395–400 (2020).
- C. R. Wells et al., Impact of international travel and border control measures on the global spread of the novel 2019 coronavirus outbreak. *Proc. Natl. Acad. Sci. U.S.A.* **117**, 7504–7509 (2020).
- C. Xiong, S. Hu, M. Yang, W. Luo, L. Zhang, Mobile device data reveal the dynamics in a positive relationship between human mobility and COVID-19 infections. *Proc. Natl. Acad. Sci. U.S.A.* **117**, 27087–27089 (2020).
- E. L. Glaeser, C. Gorbach, S. J. Redding, JUE insight: How much does COVID-19 increase with mobility? Evidence from New York and four other U.S. cities. *J. Urban Econ.* **21**, 103292 (2020).
- X. Hou et al., Intracounty modeling of COVID-19 infection with human mobility: Assessing spatial heterogeneity with business traffic, age and race. *Proc. Natl. Acad. Sci. U.S.A.* **118**, e2020524118 (2021).
- T. Gan, W. Li, L. He, J. Li, Intracity pandemic risk evaluation using mobile phone data: The case of Shanghai during COVID-19. *ISPRS Int. J. Geo-Inf.* **9**, 715 (2020).
- Wikipedia, Travel restrictions related to the COVID-19 pandemic. https://en.wikipedia.org/wiki/Travel_restrictions_related_to_the_COVID-19_pandemic. Accessed 1 September 2020.
- D. Balcan et al., Multiscale mobility networks and the spatial spreading of infectious diseases. *Proc. Natl. Acad. Sci. U.S.A.* **106**, 21484–21489 (2009).
- S. Lai et al., Effect of non-pharmaceutical interventions to contain COVID-19 in China. *Nature* **585**, 410–413 (2020).
- A. Pan et al., Association of public health interventions with the epidemiology of the COVID-19 outbreak in Wuhan, China. *J. Am. Med. Assoc.* **323**, 1915–1923 (2020).
- R. Li et al., Global COVID-19 pandemic demands joint interventions for the suppression of future waves. *Proc. Natl. Acad. Sci. U.S.A.* **117**, 26151–26157 (2020).

19. B. Rader *et al.*, Crowding and the shape of COVID-19 epidemics. *Nat. Med.* **26**, 1829–1834 (2020).
20. H. Fang, L. Wang, Y. Yang, Human mobility restrictions and the spread of the novel coronavirus (2019-nCoV) in China. *J. Publ. Econ.* **191**, 104272 (2020).
21. National Health Commission of the People's Republic of China, The latest update of the novel coronavirus pneumonia epidemic as of 24:00 on April 28. www.nhc.gov.cn/xcs/yqtb/202004/935b1804bd0d4853b898b8606279a045.shtml. Accessed 22 December 2020.
22. National Health Commission of the People's Republic of China, The latest update of the novel coronavirus pneumonia epidemic as of 24:00 on March 31. www.nhc.gov.cn/xcs/yqtb/202104/e7a8c492aa0b404e9039dd3a308bc06a.shtml. Accessed 6 April 2021.
23. Wuhan Municipal Health Commission, The latest update of the novel coronavirus pneumonia epidemic in Wuhan as of 24:00 on March 31. wjw.wuhan.gov.cn/ztl.28/fk/tzgg/202104/t202104v01.1660705.shtml. Accessed 6 April 2021.
24. J. Dehning *et al.*, Inferring change points in the spread of COVID-19 reveals the effectiveness of interventions. *Science* **15**, eabb9789 (2020).
25. L. F. Lee, J. Yu, Some recent developments in spatial panel data models. *Reg. Sci. Urban Econ.* **40**, 255–271 (2010).
26. X. Han, C. S. Hsieh, L. F. Lee, Estimation and model selection of higher-order spatial autoregressive model: An efficient Bayesian approach. *Reg. Sci. Urban Econ.* **63**, 97–120 (2017).
27. K. Li, "Spatial panel data models with structural change" (MPRA Paper No. 85388, Munich University Library, Munich, Germany, 2018).
28. T. Hu *et al.*, Building an open resources repository for COVID-19 research. *Data Inform. Manag.* **4**, 130–147 (2020).
29. European Centre for Disease Prevention and Control, Download historical data (to 14 December 2020) on the daily number of new reported COVID-19 cases and deaths worldwide. <https://www.ecdc.europa.eu/en/publications-data/download-todays-data-geographic-distribution-covid-19-cases-worldwide>. Accessed 21 June 2020.
30. S. A. Lauer *et al.*, The incubation period of coronavirus disease 2019 (COVID-19) from publicly reported confirmed cases: Estimation and application. *Ann. Intern. Med.* **172**, 577–582 (2020).
31. H. Gibbs *et al.*, Changing travel patterns in China during the early stages of the COVID-19 pandemic. *Nat. Commun.* **11**, 5012 (2020).
32. B. Li, L. Ma, Migration, transportation infrastructure, and the spatial transmission of COVID-19 in China. *J. Urban. Econ.* **15**, 103351 (2020).
33. T. Kuchler, D. Russel, J. Stroebel, "The geographic spread of COVID-19 correlates with structure of social networks as measured by Facebook" (Tech. Rep. No. w26990, National Bureau of Economic Research, Cambridge, MA, 2020).
34. T. Krizstin, P. Piribauer, M. Wögerer, The spatial econometrics of the coronavirus pandemic. *Lett. Spat. Resour. Sci.* **13**, 209–218 (2020).
35. D. Holtz, M. Zhao, S. G. Benzell, C. Y. Cao, M. A. Rahimian, Interdependence and the cost of uncoordinated responses to COVID-19. *Proc. Natl. Acad. Sci. U.S.A.* **117**, 19837–19843 (2020).
36. R. Li *et al.*, Global COVID-19 pandemic demands joint interventions for the suppression of future waves. *Proc. Natl. Acad. Sci. U.S.A.* **117**, 26151–26157 (2020).
37. X. Chen, Y. Qiu, W. Shi, P. Yu, Optimal travel restrictions in epidemics. SSRN [Preprint] (2020). <http://dx.doi.org/10.2139/ssrn.3665543> (Accessed 8 July 2021).
38. T. W. Russell *et al.*, Effect of internationally imported cases on internal spread of COVID-19: A mathematical modelling study. *Lancet Public Health* **6**, e12–e20 (2021).
39. Y. Qiu, X. Chen, W. Shi, Impacts of social and economic factors on the transmission of coronavirus disease 2019 (COVID-19) in China. *J. Popul. Econ.* **9**, 1–46 (2020).
40. H. Allcott *et al.*, "What explains temporal and geographic variation in the early US coronavirus pandemic?" (Tech. Rep. No. w27965, National Bureau of Economic Research, 2020).
41. S. Chen, Q. Li, S. Gao, Y. Kang, X. Shi, State-specific projection of COVID-19 infection in the United States and evaluation of three major control measures. *Sci. Rep.* **33**, 22429 (2020).